NJC

Accepted Manuscript

This is an *Accepted Manuscript*, which has been through the Royal Society of Chemistry peer review process and has been accepted for publication.

Accepted Manuscripts are published online shortly after acceptance, before technical editing, formatting and proof reading. Using this free service, authors can make their results available to the community, in citable form, before we publish the edited article. We will replace this *Accepted Manuscript* with the edited and formatted *Advance Article* as soon as it is available.

You can find more information about *Accepted Manuscripts* in the Information for Authors.

Please note that technical editing may introduce minor changes to the text and/or graphics, which may alter content. The journal's standard Terms & Conditions and the Ethical guidelines still apply. In no event shall the Royal Society of Chemistry be held responsible for any errors or omissions in this *Accepted Manuscript* or any consequences arising from the use of any information it contains.

ROYAL SOCIETY OF CHEMISTRY

www.rsc.org/njc

Journal Name

RSCPublishing

ARTICLE

Efficient Synthetic Supramolecular Channels and Their Light-deactivated Ion Transport in Bilayer Lipid Membranes

Cite this: DOI: 10.1039/xoxxoooooox

Received ooth January 2012,
Accepted ooth January 2012

DOI: 10.1039/xoxxoooooox

www.rsc.org/

Chunyan Bao,* Meixin Ma, Funa Meng, Qiuning Lin, and Linyong Zhu*

Inspired by the critical role of ion channel protein in regulation of cellular activities, here we developed a new kind of synthetic ion channels by simple benzocrown ether-based derivatives **M1** and **M2**, where **M1** had an dodecyl tail and **M2** had an diethylene glycol-conjugated dodecyl tail. Being their amphiphilic nature, the two small molecules were assumed to form crown ether channels through supramolecular interactions in bilayer lipid membranes (BLMs). The efficient ion transport was investigated by both a fluorescence-based vesicle assay and a planar bilayer conductance measurement, and **M2** with diethylene glycol substitution exhibited more efficient activity comparable to amphotericin B. Meanwhile, the presence of photo-sensitive *o*-nitrobenzyl group provided the light-regulation to deactivate ion transport by destroying the channel assembly of the molecules in BLMs, which provided new opportunities for developing intelligent light-regulated systems for biomedical application based on the synthetic small molecules.

Introduction

Nature ion channels are kinds of membrane proteins that mediate ions flow across plasma membranes and play essential roles for regulation of vital activities, including metabolism, signal transduction, cell proliferation and osmotic stress response.[1-5] The unique transmembrane transport behavior of the channel proteins overwhelmingly compel the chemists with great interests to develop various synthetic channels to mimic the ionic transport processes, and thus enhance understanding of how ion channels work and provide tools for many applications in life science and materials science.[6-10]

So far, typical architectures of synthetic channels can be classified into two types, namely, unimolecular and supramolecular channels. Cyclodextrins,[11] pillararene,[12,13] and helical oligomers[14,15] have been greatly used in the former models as single molecules for efficient channel transport in BLMs, while crown ethers,[16] cyclic peptides,[17] aromatic macrocycles,[18] and other supramolecular aggregates[19-23] have been applied to construct supramolecular channels. Compared to the channels constructed by unimolecular macromolecules, the utilization of supramolecular self-assembly offers simple synthesis, structural tunability and responsive functionalization to guide the formation of channels in BLMs. However, the presence of excess monomer and the participation competition of supramolecular aggregates between the solution and membrane phase greatly affect the transport efficiency, which increase the difficulty for scientists to develop diverse active supramolecular channels.[24] Thus, creation of supramolecular channels with high activity attracts more and more scientific attentions.

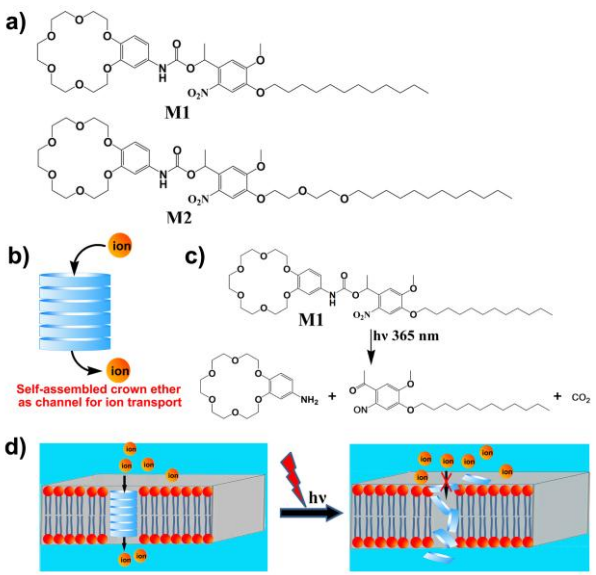

Scheme 1. Schematic representations of: a) the molecular structures, b) the proposed channel-like self-assembly of **M1** and **M2** in the BLMs, c) the photolysis mechanism of **M1**, d) the proposed light-deactivated ion transport mechanism of **M1** and **M2**.

Besides the efficient ion transport, nature ion channels are sensitive to external stimulus, including ligand,[25] potential,[26] pH[27] and light[28] stimulation. Although light-sensitive ion translocation is limited in natural occurring organisms, light-

regulated ion channel can enable the direct manipulation of cellular excitability in genetically modified cells, because cell activation can be directly linked to the diffusion of ions across the cell membrane.[29,30] Over the last few decades, many light-regulated channel proteins have been reported by using either reversible photo-switch[31-33] or irreversible photo-cage methodologies.[34-36] In contrast to the photo-switch modified channels with function of reversible-gated ion transfer, photo-caged channels are irreversible but also exhibit significant utility in biomedical areas. Ko ҫer et al. reported a *o*-nitrobenzyl modified protein to show irreversibly photo-activated channel activity,[34] while England et al. devised a variant by preparing a photo-deactivated protein channel to explore the structure and function of the channel protein.[35] Actually, while opening ion channels to activate and restore cell functions, the persistent partial activation of ion channels is not necessarily a good thing.[37] For example, an overload of Ca^{2+} from persistent influx can induce myocardial necrosis and cell apoptosis.[38] Therefore, following the efficient activation of ion transport, producing a light-induced loss of channel ability is also very important.

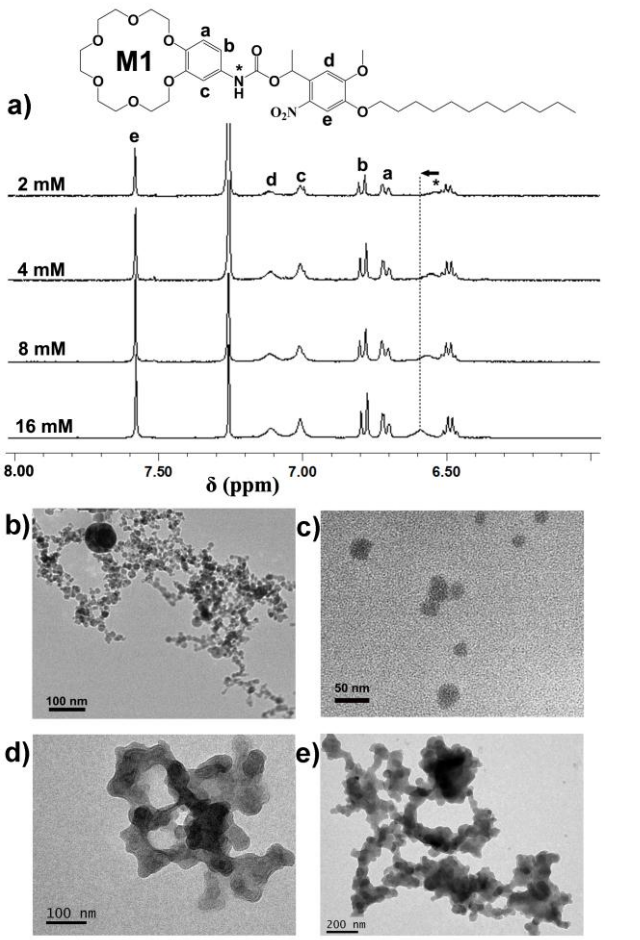

Figure 1. a) Partial ^{1}H NMR spectra for compound **M1** at different concentrations in $CDCl_3$ at 25 ^{o}C. Direct TEM observation for the morphologies of **M1** and **M2**: b) **M1** in chloroform, c) **M2** in chloroform, d) **M1** in 10 mM HEPES solution and e) **M2** in 10 mM HEPES solution. The samples of d-e) were prepared by dropping the chloroform solution into 10 mM HEPES solution.

In this paper, we designed two model molecules **M1** and **M2** (Scheme 1a) to construct efficient supramolecular ion channels in BLMs and achieve light-regulated loss of channel activity by intramolecular photocleavage. In the two channel molecules, 18-benzocrown-6 ether, a common cation-recognition moiety, was selected for potential channel stacking, and *o*-nitrobenzyl phototrigger was introduced as the photocleavage group to deactivate ion transport upon light illumination. We expected that the amphiphilic character of these molecules could provide a face-to-face assembly, which helped the formation of crown ether channel for transporting ions across BLMs efficiently (Scheme 1b). While the photo-induced cleavage in the amphiphilic building blocks would trigger disassembly of the channel molecules and disability of ion transport (Scheme 1c-1d). We envision that these unique optical deactivated ion channels, which are quite different from those reported optical activated protein channels, would possess great biomedical properties for use in sterilization, anticancer therapy and diseases treatment.

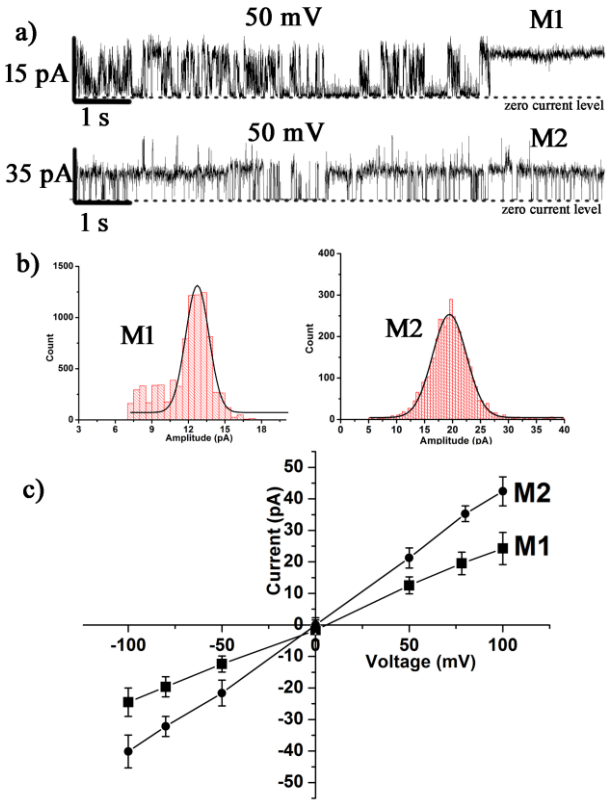

Figure 2. Bilayer planar membrane activity of compounds at 2.5 μM in a DPhPc membrane with 1 M KCl (10.0 mM HEPES, pH 7.0). a) Selected single-current signals for **M1** and **M2**, b), The corresponding current statistic histograms and Gaussian fitting of the current signal in a), c), The I-V plot using a voltage ramp from -100 mV to 100 mV.

Results and discussion

Self-assembly of Compounds M1 and M2 in Solutions

Amphiphilic compounds **M1** and **M2** were synthesized simply in several steps with high yields (Figure S1, ESI†). Because compounds **M1** and **M2** have similar backbones to our previous amphiphilic channel molecules,[39,40] we expected them to display similar channel transport mechanisms via supramolecular self-assembly of the amphiphiles. Base on the similar property of chloroform to the hydrophobic phase of membrane, the self-assembly of the molecules in chloroform

and HEPES solution was characterized by both NMR and TEM morphology investigation. The downfield shifted signal of NH protons with increasing concentrations in the concentrated NMR spectra indicated the formation of self-assembly through intermolecular H-bonding (Figure 1a, Figure S2, ESI†), the micelle-like aggregates in chloroform (Figure 1b-c) and the necklace-like fibrous aggregates in the buffer solution (Figure 1d-e) further indicated the self-assembled morphologies through intermolecular supramolecular interactions. Although no more stacking information was obtained due to the weakly self-assembled interaction and soft backbone of the compounds, it was reasonable to speculate that compounds **M1** and **M2** would also adopt columnar stacking, in which the crown ether moieties arrayed into channel-like stacking.[16,39,40]

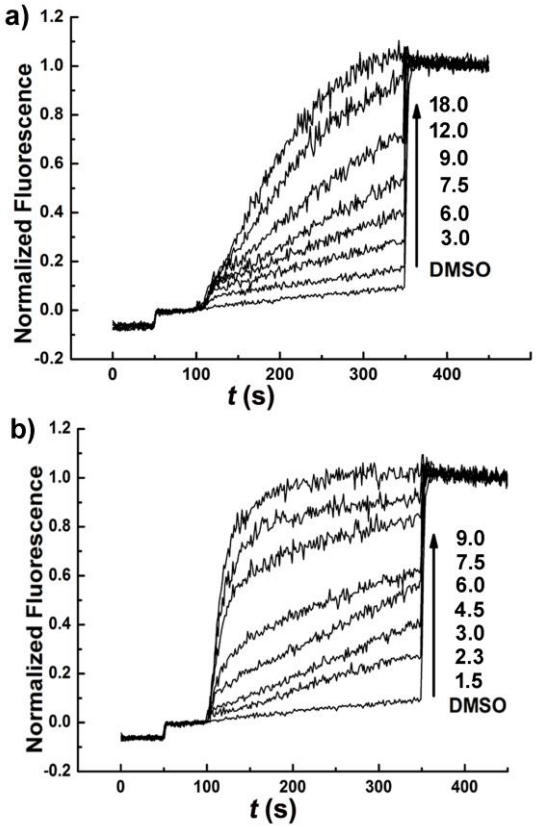

Figure 3. HPTS assays for a) **M1** and b) **M2** for K^+ transport with increasing **M1** and **M2** concentrations (final concentrations, mol% relative to lipids). Conditions: internal and external buffer (1 mM HPTS, 10 mM HEPES, 100 mM KCl, pH 7.0), external buffer (10 mM HEPES, 100 mM KCl, pH 7.0).

Channel Current Studies in Planar Lipid Bilayers

A patch-clamp technique in planar membrane was firstly applied to characterize ion transport of the synthetic ion channels, since planar bilayer conductance measurements provided diagnostic evidence for a channel mechanism.[1,24] After a short duration of membrane disruption with spikes of highly variable amplitude (not shown), both **M1** and **M2** at 2.5 μM exhibited current signals during dozens of separated experiments and the predominant signals were shown in Figure 2 (Figure S3, ESI†). Both of them exhibited single channel-like character with square-topped currents signals (Figure 2a). **M1** generated a predominant signal of 12.5 pA at 50 mV and the ohmic I-U profiles allowed evaluation of conductance as 0.25 ± 0.1 nS (nanosiemens), while **M2** had an open current signal of 20 pA at 50 mV with a specific conductance at 0.40 ± 0.1 nS (in 1 M KCl). The obtained conductance value was consistent with our previous results[39,40] and the pore size calculated from Hille equation was about 3.2 Å for **M2**, matching with the diameter of a single benzocrown ether (2.8~3.2 Å) (see ESI†).

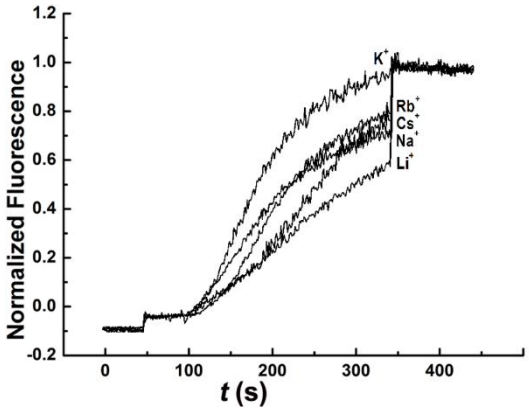

Figure 4. Assays of cation selectivity of **M1** (final concentration, 18.0 mol%). Conditions: internal buffer (1 mM HPTS, 10 mM HEPES, 100 mM KCl, pH 7.0), external buffer (10 mM HEPES, 100 mM MCl, pH 7.0).

Ion Transporting Activity Studies by Vesicle Assays

Then, a 8-hydroxy-1,3,6-pyrenetrisulfonate (HPTS) labelled LUV fluorescence assay was carried out to explore the transport activity of the channels.[24,39] In this assay, the ion transport through the membranes was accessed by the change in ratio fluorescence intensity at 510 nm (I_{450}/I_{405}) of the pH-sensitive HPTS dye entrapped inside the vesicles. A pH gradient across the vesicle membrane was introduced by addition of base (alkali hydroxide), and then the addition of channel molecules to these vesicles led to the antiport of H^+/K^+ or the synport of K^+/OH^-, thus induced the changes in HPTS emission. For each set of experiments, the final concentration of the lipids in the experiments was a constant at 33 μM (assuming 100% of lipids were incorporated into liposomes). As shown in Figure 3a, a variation in the concentration of **M1** induced a corresponding change in the transmembrane activity, suggesting successful permeability to ions. Compound **M2** exhibited similar, but more efficient transmembrane activity (Figure 3b), arriving 1.0 at concentration of 9.0 mol% (18.0 mol% for **M1**). To quantitatively compare the transmembrane activities of the amphiphiles, the transport activity EC_{50} (concentration of transport required to achieve 50% activity) and Hill coefficient n value were determined from the dose response curves (Figure S4, ESI†). **M2** had an EC_{50} value at 3.38 mol%, while **M1** had an EC_{50} value of 10.26 mol% (~ 3 times more active than **M1**). Meanwhile, the nonlinear relationship between transmembranne acitivities and concentrations further suggested the channel-like ion transport of amphiphilic molecules **M1** and **M2** in lipid bilayers. Since 18-benzocrown-6 ether has selective recognition with K^+, the transmembrane activity with different cations was explored. As shown in Figure 4, M1 exhibited a slight preference for transporting K^+ over Rb^+, Cs^+, Na^+ and Li^+. All these suggested the ion transport of the compounds should be due to the channel formation by crown ether stacking and not through undefined

perturbation or pores created by the other constituents of the molecules (as illustrated in Scheme 1b).

To illustrate efficient ion transport of **M1** and **M2**, amphotericin B, a commercial channel antibiotic, was analyzed using HTPS transmembrane activity assay under the same conditions (Figure S5, ESI†). Similarly, the transmembrane activity of amphotericin B increased as a function of concentrations, and arrived a maximum activity of ~ 0.8 at 181.8 mol% with EC_{50} ≈ 3.0 mol%. The comparable transmembrane activity to amphotericin B suggested that both **M1** and **M2** possessed excellent ion transport activity across BLMs, and **M2** was especially effective due to its diethylene glycol substitution. To clarify the improved transmembrane activity of **M2** compared to **M1**, the solubility of the compounds in buffer solution and their doping amounts in the BLMs were determined.[39] Unexpectedly, the compounds exhibited similar solubility (> 80 μM, Figure S6, ESI†) and doping amount within the BLMs (~ 70%, Figure S7, ESI†). Combining with the similar association constants with K^+ ions of **M1** and **M2** (Table S1, ESI†), the improved transmembrane activity of **M2** should be attributed to the different ion-dipole interactions by way of the diethylene glycol substitution (Figure S8, ESI†).[41,42]

Photo-deactivated Ion Transport

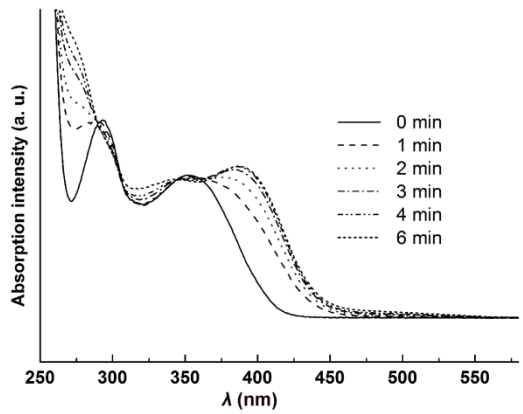

Figure 5. Evolution of the UV-Vis absorption spectra of **M1** (6.0 μM in DMSO with microcuvette) as a function of the irradiation with a 365 nm LED lamp at 30 $mWcm^{-2}$.

The photolysis process of **M1** was detected by evolution of UV-vis absorption signal. As shown in Figure 5, with an increase in irradiation time, the absorption band at 358 nm decreases, which is accompanied by the appearance of a band at 380 nm, indicating the photo-cleavage of **M1** into its products.[43] The generation of isosbestic points at 288, 303, and 346 nm indicates a relatively clean photochemical reaction for **M1** upon irradiation. The photolysis products of **M1** and **M2** were verified by the ^1H NMR and HPLC spectra (Figure S9-10, ESI†), including one molecule of parent 4-amino-benzocrown ether, carbon dioxide, and the corresponding nitroso ketone derivative (Scheme 1c). Accompanying with the successful photolysis, the self-assembly of the molecules was also disrupt as confirmed by the collapse TEM morphologies (Figure S11, ESI†). Knowing that efficient ion transport of the amphiphiles was triggered by a supramolecular channel mechanism, the light-induced destroy of the assembly in both solution and BLMs would deactivate the ion transport, as illustrated in Scheme 1d.

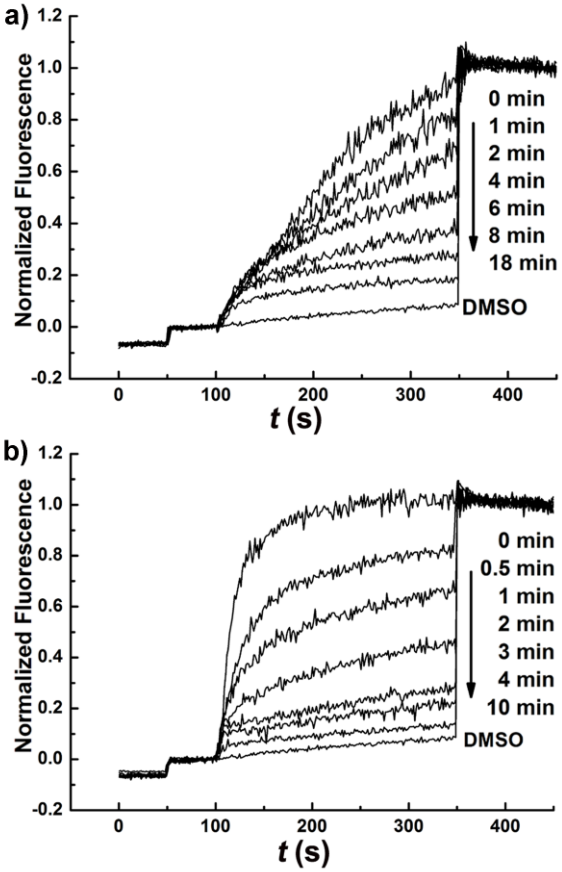

Figure 6. Observed change in transmembrane activity when a) **M1** (18.0 mol%, final concentration) and b) **M2** (9.0 mol%, final concentration) were photo-cleaved by irradiation at 365 nm UV light (30 $mWcm^{-2}$).

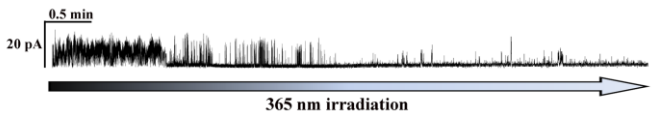

Figure 7. In situ photo-regulation of current signal of **M1** for the ion transport on the planar BLMs at 50 mV.

The photo-deactivated ion transport of the molecules in BLMs was investigated by HPTS assays. A 365 nm LED lamp with an intensity of 30 $mWcm^{-2}$ was used to irradiate the DMSO stock solutions containing the compounds. Aliquots that were irradiated for certain time intervals were used for the assay. To optimize the photo-regulation of transmembrane activity, 18.0 mol% **M1** and 9.0 mol% **M2** were applied based on their maximum transport ability at these concentrations. As shown in Figure 6, the transmembrane activity for both of compounds decreased rapidly upon irradiation of 365 nm UV light, and reached a minimum after ten minutes. Upon irradiation, **M1** displayed a significant decrease in transmembrane activity, decreasing from 0.97 to 0.09 (deducting the DMSO background, Figure 6a), while **M2** displayed an even more rapid decrease from 1.00 to 0.05 (deducting the DMSO background, Figure 6b). The activity variation before and after 365 nm irradiation at different concentrations was also measured (Figure S12, ESI†). It

suggested that the photo-irradiation significantly decreased the transport activities of the compounds.

To quantitatively compare the regulated ion transport before and after light irradiation, the transmembrane activity of the main photolysis products, 4-amino-18-benzocrown-6 ether, was detected (Figure S13, ESI†). There was a linear relationship between activity and concentrations, with an $EC_{50} > 2.2 \times 10^3$ mol%, which was much higher than the EC_{50} of **M1** and **M2** by a factor of 10^3, suggesting the carrier transport of the photolysis product with significantly lower activity and providing the determinate reason for the significantly decreased transport activity of photo-irradiated **M1** and **M2**. The photo-deactivated ion transport was also confirmed by in situ photo-regulation of compound **M1** on a planar BLMs (Figure 7). Upon irradiation at 365 nm, the frequency of the open current signal was significantly reduced and even disappeared after several minutes.

Conclusions

In conclusion, we developed a new class of supramolecular synthetic ion channels based on the structurally simple amphiphilic molecules **M1** and **M2**. The 8-hydroxy-1,3,6-pyrenetrisulfonate (HPTS) fluorescence assay and the patch-clamp current experiment revealed that both of the amphiphiles possessed efficient ion channel transmembrane activity across the bilayer lipid membranes, **M2** was especially active with comparable activity to amphotericin B because of its diethylene glycol substitution. Upon light irradiation, there were deformation of the self-assembled channel and generation of photolysis products with three orders of magnitude lower transport activity, producing the light-regulated deactivation of ion transport. These readily availability of small molecules can be used to easily regulate ion transport via light illumination.

Experimental Section

Materials. All starting materials were obtained from commercial suppliers and were used without further purification unless otherwise stated. All air- or moisture-sensitive reactions were performed using oven-dried or flame-dried glassware under an inert atmosphere of dry argon. Air- or moisture-sensitive liquids and solutions were transferred via syringe. Egg yolk phosphatidylcholine (EYPC) was obtained from Avanti Polar lipids as a solution in chloroform (25 mg mL^{-1}). 8-hydroxy-1,3,6-pyrenetrisulfonate (HPTS) and Trixon-100 were obtained from Sigma-Aldrich and used without further purification.

Characterizations. Proton and carbon nuclear magnetic resonance spectra (^1H, ^{13}C NMR) were recorded on a Bruker Avance 500 (400 MHz) spectrometer. Chemical shifts were reported in parts per million (ppm) downfield from the Me_4Si resonance which was used as the internal standard when recording ^1H NMR spectra. Mass spectra were recorded on a Micromass GCTTM and a Micromass LCTTM. Fluorescence measurements were performed on a Varian Cary Eclipses fluorescence spectrometer equipped with a stirrer and a temperature controller (kept at 25 ℃ unless otherwise noted). Absorption spectra were recorded on a Shimadzu UV-2550 UV-vis spectrometer. A Mini-Extruder used for the preparation of large unilamellar vesicles (LUVs) was purchased from Avanti Polar lipids. The size of EYPC vesicles was determined using a Delsa™ Nano Submicron Particle Size and Zeta Potential Particle Analyzer (Beckman Coulter Inc., USA). A 365 nm LED lamp (30 $mWcm^{-2}$) was used for photolysis of compounds and photo-controlled experiments.
Detailed synthesis method and partial experimental datas were described in the supporting information.

Acknowledgements

This work was supported by NSFC (51273064, 21472044), Innovation Program of Shanghai Municipal Education Commission and Fundamental Research Funds for the Central University.

Notes and references

Key Laboratory for Advanced Materials, Institute of Fine Chemicals, East China University of Science and Technology, 130# Meilong Road, Shanghai, 200237, P. R. China. Fax: (+86)-21-64253742
E-mail: baochunyan@ecust.edu.cn; linyongzhu@ecust.edu.cn
Electronic Supplementary Information (ESI) available: The detailed synthesis and characterizations of compounds, self-assembled properties, some HPTS assays, doping and solubility measurements, etc. See DOI: 10.1039/b000000x/

1 B. Hille, in *Ion channels of excitable membranes*. Sinauer Sunderland, MA, 2001.
2 C. G. Nichols, *Nature*, 2006, **440**, 470.
3 L. D. Mosgaard and T. Heimburg, *Acc. Chem. Res.*, 2013, **46**, 2966.
4 F. Lang, M. Föller, K. S. Lang, P. A. Lang, M. Ritter, E. Gulbins, A. Vereninov and S. M. Huber, *J. Membrane Biol.*, 2005, **205**, 147.
5 M. N. Phan, H. A. Leddy, B. J. Votta, S. Kumar, D. S. Levy, D. B. Lipshutz, S. H. Lee, W. Liedtke and F. Guilak, *Arthritis Rheum.*, 2009, **60**, 3028.
6 G. W. Gokel and S. Negin, *Acc. Chem. Res.*, 2013, **46**, 2824.
7 X. Hou, W. Guo and L. Jiang, *Chem. Soc. Rev.*, 2011, **40**, 2385.
8 N. Sakai and S. Matile, *Langmuir*, 2013, **29**, 9031.
9 S. J. Webb, *Acc. Chem. Res.*, 2013, **46**, 2878.
10 J. K. W. Chui and T. M. Fyles, *Chem. Soc. Rev.*, 2012, **41**, 148.
11 N. Madhavan, E. C. Robert and Mary S. Gin, *Angew. Chem. Int. Ed.*, 2005, **44**, 7584.
12 W. Si, Z. T. Li and J. L. Hou, *Angew. Chem. Int. Ed.*, 2014, **53**, 4578.
13 X.-B. Hu, Z. Chen, G. Tang, J.-L. Hou and Z.-T. Li, *J. Am. Chem. Soc.*, 2012, **134**, 8384.
14 P. Xin, P. Zhu, P. Su, J. L. Hou and Z. T. Li, *J. Am. Chem. Soc.*, 2014, **136**, 13078.
15 P. D. U. Koert, *Phys. Chem. Chem. Phys.*, 2005, **7**, 1501.
16 A. Cazacu, C. Tong, A. van der Lee, T. M. Fyles and M. Barboiu, *J. Am. Chem. Soc.*, 2006, **128**, 9541.
17 J. Sanchez-Quesada, M. P. Isler and M. R. Ghadiri, *J. Am. Chem. Soc.*, 2002, **124**, 10004.
18 X. Zhou, G. Liu, K. Yamato, Y. Shen, R. Cheng, X. Wei, W. Bai, Y. Gao, H. Li, Y. Liu, F. Liu, D. M. Czajkowsky, J. Wang, M. J. Dabney, Z. Cai, J. Hu, F. V. Bright, L. He, X. C. Zeng, Z. Shao and B. Gong, *Nat. Commun.*, 2012, **3**, 949.
19 H. Zhao, S. Sheng, Y. Hong and H. Zeng, *J. Am. Chem. Soc.*, 2014, **136**, 14270.

20 T. Muraoka, T. Endo, K. V. Tabata, H. Noji, S. Nagatoishi, K. Tsumoto, R. Li and K. Kinbara, *J. Am. Chem. Soc.*, 2014, **136**, 15584.
21 T. Saha, S. Dasari, D. Tewari, A. Prathap, K. M. Sureshan, A. K. Bera, A. Mukherjee and P. Talukdar, *J. Am. Chem. Soc.*, 2014, **136**, 14128.
22 N. Yoshino, A. Satake and Y. Kobuke, *Angew. Chem. Int. Ed.*, 2001, **40**, 457-459.
23 W.-H. Chen, M. Nishikawa, S.-D. Tan, M. Yamamura, A. Satake and Y. Kobuke, *Chem. Commun.*, 2004, 872-873.
24 S. Matile, and N. Sakai, in *Analytical Methods in Supramolecular Chemistry*. ed. C. A. Schalley, Wiley-VCH, Weinheim, 2007, pp. 391.
25 T. M. Fyles and C. C. Tong, *New J. Chem.*, 2007, **31**, 655.
26 M. Tarek and L. Delemotte, *Acc. Chem. Res.*, 2013, **46**, 2755.
27 R. Reyes, F. Duprat, F. Lesage, M. Fink, M. Salinas, N. Farman and M. Lazdunski, *J. Biol. Chem.*, 1998, **273**, 30863.
28 F. Schneider, D. Gradmann and P. Hegemann, *Biophys. J.*, 2013, **105**, 91.
29 R. J. Thompson, M. F. Jackson, M. E. Olah, R. L. Rungta, D. J. Hines, M. A. Beazely, J. F. MacDonald and B. A. MacVicar, *Science*, 2008, **322**, 1555.
30 S. Sundelacruz, M. Levin, and D. L. Kaplan, *Stem Cell Rev. Rep.*, 2009, **5**, 231.
31 M. R. Banghart, M. Volgraf and D. Trauner, *Biochemistry*, 2006, **45**, 15129.
32 T. Fehrentz, M. Schönberger and D. Trauner, *Angew. Chem. Int. Ed.*, 2011, **50**, 12156.
33 P. Osman, S. Martin, D. Milojevic, C. Tansey and F. Separovic, *Langmuir*, 1998, **14**, 4238.
34 A. Koçer, M. Walko, W. Meijberg and B. L. Feringa, *Science*, 2005, **309**, 755.
35 P. M. England, H. A. Lester, N. Davidson and D. A. Dougherty, *Proc. Natl. Acad. Sci.*, 1997, **94**, 11025.
36 M. Goeldner, R. Givens, in *Dynamic Studies in Biology*. Wiley-VCH, Weinhein, Germany, 2005.
37 E. P. Hoffman, F. Lehmann-Horn and R. Rüdel, *Cell*, 1995, **80**, 681.
38 X. Chen, X. Huang, H. Kubo, D. M. Harris, G. D. Mills, J. Moyer, R. Berretta, S. T. Potts, J. D. Marsh, and S. R. Houser, *Circ. Res.*, 2005, **97**, 1009.
39 T. Liu, C. Bao, H. Wang, Y. Lin, H. Jia, and L. Zhu, *Chem. Commun.*, 2013, **49**, 10311.
40 T. Liu, C. Bao, H. Wang, L. Fei, R. Yang, Y. Long, and L. Zhu, *New J. Chem.*, 2014, **38**, 3507.
41 O. S. Andersen, D. V. Greathouse, L. L. Providence, M. D. Becker and R. E. Koeppe, *J. Am. Chem. Soc.*, 1998, **120**, 5142.
42 D. D. Busath, C. D. Thulin, R. W. Hendershot, L. R. Phillips, P. Maughan, C. D. Cole, N. C. Bingham, S. Morrison, L. C. Baird, R. J. Hendershot, M. Cotten and T. A. Cross, *Biophys. J.*, 1998, **75**, 2830.
43 O. D. Fedoryak, J.-Y. Sul, P. G. Haydon, G. C. R. Ellis-Davies, *Chem. Commun.*, 2005, **29**, 3664.